Order by Static Disorder in the Ising Chain Magnet $Ca_3Co_{2-x}Mn_xO_6$

V. Kiryukhin,[1] Seongsu Lee,[1,2] W. Ratcliff II,[3] Q. Huang,[3] H. T. Yi,[1] Y. J. Choi,[1] and S-W. Cheong[1]

[1]*Department of Physics and Astronomy and Rutgers Center for Emergent Materials, Rutgers University, Piscataway, New Jersey 08854, USA*

[2]*Neutron Science Division, Korea Atomic Energy Research Institute, Daejeon 305-353, Korea*

[3]*NIST Center for Neutron Research, NIST, Gaithersburg, Maryland 20899, USA*

(Received 31 January 2009; published 5 May 2009)

Ising chain compound $Ca_3Co_{2-x}Mn_xO_6$ exhibits up-up-down-down long-range magnetic order (LRO) in a broad range of $0.75 < x < 1$. The LRO is abruptly lost in the narrow vicinity of $x = 1$, and the magnetic state becomes incommensurate. The commensurate state (but not the LRO) is recovered for larger x. This is surprising because the stoichiometric $x = 1$ state exhibits the best Co/Mn ionic order, and the magnetic LRO appears only in the samples with reduced ionic order. We argue that this ''order-by-static-disorder'' phenomenon may be related to the disruption of the long-range magnetic interactions by the magnetic-site disorder, reducing magnetic frustration.

DOI: 10.1103/PhysRevLett.102.187202 PACS numbers: 75.30.Kz, 75.10.Pq, 75.30.Hx, 75.40.Cx

Disorder is ubiquitous in solids. Usually, it manifests itself as defects and impurities that break the ideal crystalline order. Magnetic systems provide a rich field for investigation of the disorder effects. As in other solid-state systems, defects usually break magnetic long-range order (LRO), giving rise to various disordered states, such as cluster and spin glasses [1]. On the other hand, dynamic disorder induced by thermal fluctuations promotes magnetic order in certain degenerate systems through entropic selection of the states with the highest density of low-energy excitations [2]. This phenomenon is referred to as ''order by disorder.'' While related effects of static disorder have been discussed theoretically [3], static disorder is not known to induce magnetic LRO in the extant materials. Discovery of any experimental system exhibiting such a counterintuitive effect, possibly driven by a different mechanism, would be clearly of interest. Herein, we present a study of a magnetic system in which an unusual order-by-static-disorder phenomenon is apparently realized.

Disorder plays a particularly important role in quasi-one-dimensional (1D) magnets, where its effects are intrinsically large. Even in the simplest case of Ising spin chains, surprisingly rich phase diagrams are found when competing interactions exist. Perhaps the best known example is the axial next-nearest neighbor Ising model with nearest-neighbor (NN) ferromagnetic (FM) and next-nearest-neighbor (NNN) antiferromagnetic interactions [4]. An extension of this model on the chain of alternating Ising spins of different magnitude, the so-called alternating-spin Ising ferrimagnet (ASIF), has also been considered [5]. Because of their low dimensionality, these model systems are strongly affected by disorder, which makes them particularly useful for combined theoretical and experimental studies of disorder in magnets. Unfortunately, experimental realizations of these models are rare, and large regions of the model parameter space remain unexplored experimentally.

$Ca_3Co_{2-x}Mn_xO_6$ is a quasi-1D Ising chain compound in which c-axis Co/Mn magnetic chains form a triangular lattice in the ab plane, with three chains per unit cell as shown in Fig. 1. The strong 1D magnetic character of $Ca_3Co_{2-x}Mn_xO_6$ is well established [6,7]. The two types of oxygen cages surrounding the magnetic ions—octahedral and prismatic—alternate along the chain direction. Mn ions have a strong tendency to occupy the octahedral sites, and the $x \approx 1$ compounds contain chains of alternating Mn^{4+} and Co^{2+} ions. For $x = 0.95$, the in-chain magnetic order is of the up-up-down-down type, and the Mn and Co spins are $S = 3/2$ and $s = 1/2$, respectively, based on neutron diffraction data [7]. The $x \approx 1$ compound therefore provides a testing ground for investigation of the ASIF model and its extensions, including effects of disorder. The

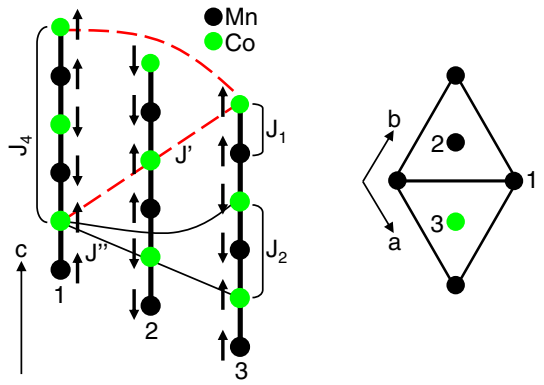

FIG. 1 (color online). Magnetic chains in Ca_3CoMnO_6. Arrows show spins in the commensurate state. The three magnetic chains on the left form an equilateral triangle, as shown in the sketch of the unit cell at right. Only Co and Mn ions are shown.

stoichiometric $x = 1$ system is expected to be the cleanest realization of the ASIF model because of the least amount of the ionic disorder (ideally, a perfect alternating chain). However, the $x = 1$ compound has not been studied in detail thus far. In this Letter, we explore such samples. Surprisingly, we find that the $x = 1$ system exhibits a much less ordered magnetic state than the compounds with ionic disorder. In other words, the ionic disorder appears to promote the magnetic LRO—a phenomenon that can be befittingly referred to as "order by static disorder."

$Ca_3Co_{2-x}Mn_xO_6$ polycrystals were prepared by solid-state reaction technique. Single crystals were grown using a KCl-K_2CO_3 flux method [7]. Magnetization was measured in zero-field cooled samples using a SQUID magnetometer. Neutron powder diffraction was performed at the BT1 beam line at NCNR using monochromatic neutrons of $\lambda = 2.079$ Å. The data were refined using the FULLPROF [8] program package. Single-crystal neutron diffraction was done in the $(H0L)$ zone at the BT9 triple-axis spectrometer at an energy of 14.7 meV, pyrolytic graphite filters before and after the sample, and 40-47-s-40-80 collimations.

Figure 2(a) shows temperature-dependent magnetization. It exhibits a broad peak at $T = T_{max}$ associated with the appearance of the magnetic order [7]. In our samples, T_{max} decreases with increasing Mn concentration x [see the inset in Fig. 2(a)]. All the samples exhibit sharp nuclear peaks in neutron powder diffraction patterns characteristic to well-ordered nuclear structure. Table I shows selected results of the Rietveld refinement of the nuclear structure for the samples with $x \approx 1$. The data were taken above the magnetic ordering temperature at $T = 20$ K. Excellent agreement factors are achieved. Importantly, the stoichiometric $x = 1$ sample exhibits a perfect ionic order with Co and Mn occupying the trigonal and the octahedral sites, respectively. The data and the Rietveld refinement for this sample are shown in Fig. 3(a). The other samples exhibit ionic disorder (octahedral Co or trigonal Mn) in good agreement with their nominal compositions. In contrast to the nuclear structure, the magnetic order exhibits dramatic changes in the narrow vicinity of $x = 1$. Figure 3(b) shows scans through the (101) magnetic peak position for $T = 1.4$ K, which is much smaller than T_{max}. While the $x = 0.75$ and $x = 0.95$ samples exhibit resolution-limited magnetic peaks and the associated magnetic LRO, the magnetic peaks broaden significantly for $x = 1$, signaling the loss of the LRO. Moreover, the peak shifts from the (101) position, and therefore the magnetic structure becomes incommensurate (IC). When x is further increased to 1.05, the commensurate state is recovered. In addition, the magnetic peak appears to narrow down, although the LRO is clearly not restored. We stress that no anomalies in the nuclear structure are associated with these changes.

To study the characteristics of the IC state in more detail, single crystals were investigated. Samples with low nominal Mn concentrations x exhibit sharp commensurate (101) peaks. With increasing x, the peaks broaden and become IC in the direction of the magnetic chains, L. The $(10L)$ scan through the magnetic peak in the sample with the largest x

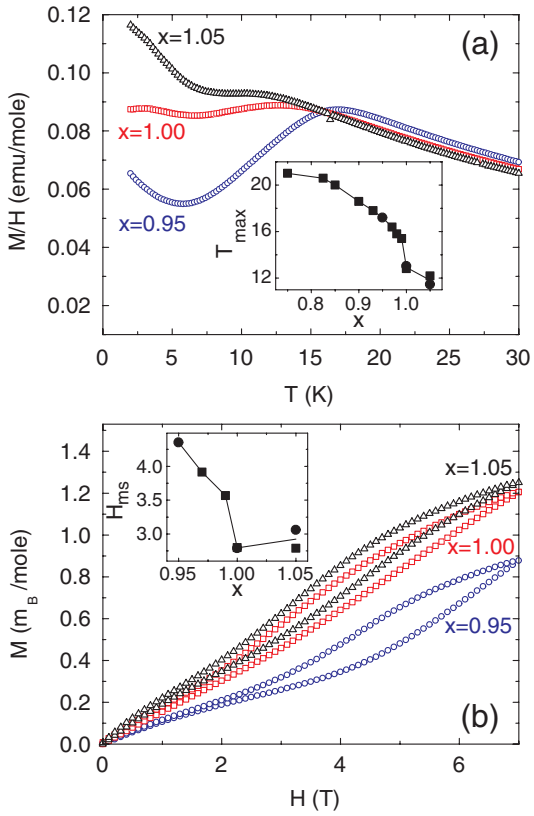

FIG. 2 (color online). (a) Temperature dependence of the magnetic susceptibility of zero-field cooled $Ca_3Co_{2-x}Mn_xO_6$. It exhibits a broad peak at $T = T_{max}$, which is shown in the inset as a function of x. The magnetic field is 0.2 T. (b) Magnetization of zero-field cooled samples versus magnetic field for $T = 2$ K. The magnetic field H_{ms} at which M exhibits the maximum slope on decreasing the field is shown in the inset as a function of x. The main panels, as well as the circles in the insets, show the data for the samples studied by neutron diffraction (see the text for details). Lines are guides to eye.

TABLE I. Nominal and experimental occupation factors for the trigonal and octahedral Co/Mn sites, as determined by Rietveld analysis. Experimental errors are in parentheses. The occupation factors marked with (f) reached the maximum allowed value of 1 and were fixed at 1. Agreement factors R-Bragg are also shown.

x		Trig. Co	Oct. Mn	Trig. Mn	Oct. Co	R
0.95	Nom.	1	0.95	0	0.05	
	Exp.	1(f)	0.954(4)	0(0.04)	0(0.0001)	0.0214
1.00	Nom.	1	1	0	0	
	Exp.	1.003(2)	1.003(2)	0(0.0003)	0(0.0003)	0.0224
1.05	Nom.	0.95	1	0.05	0	
	Exp.	0.973(7)	1(f)	0(0.0001)	0(0.03)	0.0238

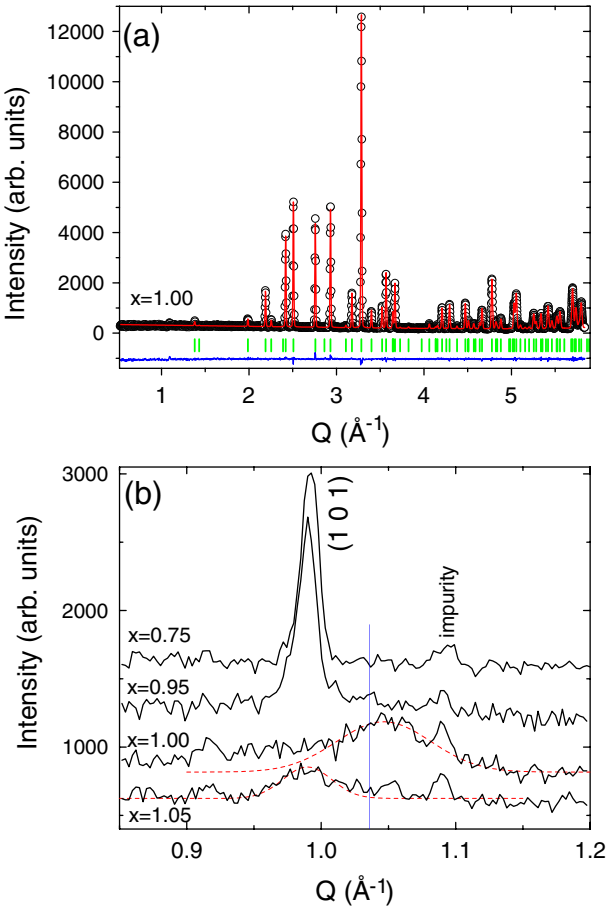

FIG. 3 (color online). (a) Observed (symbols) and calculated (line) powder neutron diffraction patterns for the $x = 1$ sample for $T = 20$ K. The bars show the nuclear Bragg peak positions, and the line at the bottom is the difference between the observed and calculated patterns. (b) Powder diffraction patterns in the vicinity of the (101) magnetic peak for $T = 1.4$ K for various values of x. Vertical solid line shows the Q of the magnetic peak of the single-crystal sample of Fig. 4. Dashed lines are guides to eye.

obtained is shown in Fig. 4 for $T = 5$ K. The Gaussian fit, shown with the dashed line, gives $L = 1.11(0.01)$ reciprocal lattice units (r.l.u.) for this sample. Comparison of this wave vector [the vertical line in Fig. 3(b)] with those of the powder samples suggests that x is within a few percent of $x = 1$. The in-chain correlation length, defined as inverse half width at half maximum of the Gaussian fit, is $\xi = 19(3)$ Å. Both the incommensurability, $\Delta L \equiv L - 1$, and ξ do not depend on temperature within the experimental accuracy, 40% for ΔL and 20% for ξ. The temperature dependence of the peak intensity is shown in the inset in Fig. 4. The intensity is from Gaussian fits; the peak width was fixed at the low-temperature value for $T > 8$ K. The obtained magnetic transition temperature is in agreement with the anomalies in the magnetic susceptibility in the large-x samples of Fig. 2(a). Unfortunately, because of the

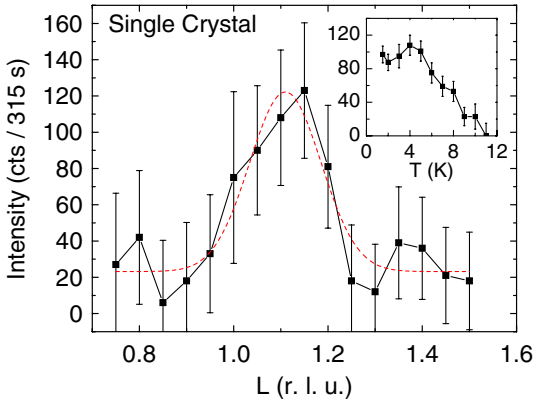

FIG. 4 (color online). L scan through the (10L) magnetic peak in the single-crystal sample described in the text, $T = 5$ K. The dashed line shows the Gaussian fit. The temperature dependence of the peak intensity is shown in the inset. Error bars are from counting statistics.

nature of the flux-growth technique, the compositions of the single crystals are not known with the accuracy required to address the $x = 1$ anomaly discussed above.

The abrupt changes in the microscopic magnetic structure in the vicinity of $x = 1$ are reflected in the bulk magnetic properties. First, as shown in the inset in Fig. 2(a), T_{max} exhibits a sharp drop with increasing x at $x = 1$. This observation is consistent with the suppression of the magnetic LRO at $x = 1$. The second effect is associated with sensitivity of the system to an applied magnetic field, H. Figure 2(b) shows field dependence of the magnetization M on increasing and decreasing the field in the magnetically ordered state ($T = 2$ K). The change of the slope of this dependence is due to the onset of the gradual transition to the state with the up-up-up-down spin order [9]. The field of the maximum slope of $M(H)$ on decreasing the field, H_{ms}, is shown in the inset in Fig. 2(b). It exhibits a large drop with increasing x at $x = 1$, followed by stabilization or even a small increase for $x > 1$. Numerous imperfections in the magnetic order in the short-range ordered state produce local segments of the up-up-up-down order and provide nucleation centers for the field-induced transition. This effect should lower the transition onset field in the poorly ordered samples. Therefore, the observed behavior of H_{ms} is consistent with the destruction of the LRO at $x = 1$, as well as with a possible partial recovery of the magnetic order for higher values of x, as observed in neutron diffraction experiments. To confirm the anomalous features of the $x = 1$ and $x = 1.05$ compositions, measurements with two independently prepared sets of samples were performed. One of these sets (circles in the insets in Fig. 2) was used for neutron experiments. While there is a certain variation for $x = 1.05$, the data of Fig. 2 clearly demonstrate that the bulk magnetic properties exhibit an anomaly at $x = 1$, providing a strong argument for the uniqueness of this composition.

The above data show that the magnetic LRO disappears and the magnetic state becomes IC in a narrow vicinity of $x = 1$ with almost perfect ionic order. This observation is highly surprising because the LRO appears to be stabilized by the ionic disorder in a wide range of Mn concentrations $x < 1$, providing an intriguing example of the order by disorder phenomenon. Moreover, the neutron diffraction measurements indicate that $x = 1$ is a special point in this system, at which the incommensurability is largest and the magnetic order is poorest, contrary to usual expectations. The bulk magnetic properties of Fig. 2 are consistent with this conclusion.

To shed light on this behavior, knowledge of the magnetic couplings is necessary. Unfortunately, the small size of the available crystals prevents determination of these couplings using inelastic neutron scattering. Lacking such information, one can still obtain a useful insight by assessing their relative importance using the crystal structure. The in-chain NN and NNN interactions J_1 and J_2 (Fig. 1) are probably the largest. For our discussion, the difference between the Co-Co and Mn-Mn interactions is ignored for simplicity. If only these interactions are considered, only two ground states are possible in both the axial NNN Ising and ASIF models in the case of FM NN interaction suggested in [7]: the experimental up-up-down-down and the FM state [4,5]. The effective Curie temperature of this system grows with decreasing x, and the $x = 0$ chains are ferromagnetic [6]. Thus, increasing x in the vicinity of $x = 1$ moves the system deeper into the up-up-down-down state and cannot account for its destabilization. Even if the NN interaction is antiferromagnetic, as alternatively proposed in [10], the above models cannot explain the clear anomaly at $x = 1$ observed in our experiments. To understand this effect, longer-range interactions must therefore be considered. The interchain superexchange path is most favorable [11] for the NNN Co-Co antiferromagnetic interaction J' (Fig. 1) which forms an infinite spiral along the three adjacent chains. Given the existing in-chain order, this path is geometrically frustrated in the same manner as the 2D Ising triangular lattice. Because of this frustration, the interchain magnetic structure appears to be set by a different interaction path, J'', which lacks frustration and also forms a spiral but with a shorter pitch. This structure is destabilized by the long-range effective coupling J_4 arising from the frustrated path J'. In systems with large uniaxial anisotropy this type of competing interaction is associated with longitudinal sinusoidally modulated structures. It may, therefore, give rise to the IC state in our samples. Note that a similar mechanism was proposed to explain the long-wavelength IC modulation in the FM Ising chains for $x = 0$ [12]. Competing interactions may also be responsible for the destruction of the LRO in the IC state through, for example, creation of regions with low spin density in the modulated chains, and by affecting the frustrated interchain interactions. Long-range interactions with complex paths such as J_4 are strongly affected by disorder, and it is possible that the ionic disorder is sufficient to disrupt this interaction path everywhere except for the small vicinity of $x = 1$, where the IC state is observed. The commensurate state, with LRO for $x < 1$, is realized in the more disordered samples with suppressed competing interactions, giving rise to the apparent order by disorder phenomenon.

Clearly, other explanations are possible at this stage. The triangular motif of the crystal lattice suggests the importance of geometric frustration, which often leads to magnetic disorder, especially in Ising systems. In nonmagnetic systems, impurities may lift the frustration, thereby giving rise to an ordered state. One example of such an effect is suppression of the Pauling disorder in H_2O ice by KOH dilution [13]. We note, however, that spin vacancies do not induce the LRO in the 2D Ising triangular lattice [14], neither do they in pyrochlore spin ices [15], and we are not aware of any Ising magnetic system showing this effect. Experimental determination of the magnetic couplings, as well as theoretical research, are clearly needed to understand this system. $Ca_3Co_{1-x}Mn_xO_6$ is a rare realization of a quasi-1D alternating-spin Ising system with geometrically frustrated interchain interaction, which also exhibits ferroelectricity and unusual field-induced transitions [7,9]. Our measurements reveal another intriguing phenomenon in this system: a magnetic long-range order that is apparently promoted by magnetic-site disorder.

This work was supported by the DOE under Grant No. DE-FG02-07ER46382.

[1] J. A. Mydosh, *Spin Glasses. An Experimental Introduction* (Taylor and Francis, London, 1993).
[2] J. Villain *et al.*, J. Phys. (Paris) **41**, 1263 (1980).
[3] C. L. Henley, J. Appl. Phys. **61**, 3962 (1987).
[4] P. Bak, Rep. Prog. Phys. **45**, 587 (1982).
[5] J.-J. Kim, S. Mori, and I. Harada, J. Phys. Soc. Jpn. **65**, 2624 (1996).
[6] S. Aasland, H. Fjellvag, and B. Hauback, Solid State Commun. **101**, 187 (1997).
[7] Y. J. Choi *et al.*, Phys. Rev. Lett. **100**, 047601 (2008).
[8] J. Rodriguez-Carvajal, Physica (Amsterdam) **192B**, 55 (1993).
[9] Y. J. Jo *et al.*, Phys. Rev. B **79**, 012407 (2009).
[10] H. Wu *et al.*, Phys. Rev. Lett. **102**, 026404 (2009).
[11] R. Frésard *et al.*, Phys. Rev. B **69**, 140405(R) (2004).
[12] S. Agrestini *et al.*, Phys. Rev. Lett. **101**, 097207 (2008).
[13] Y. Tajima, T. Matsuo, and H. Suga, Nature (London) **299**, 810 (1982).
[14] G. S. Grest and E. G. Gabl, Phys. Rev. Lett. **43**, 1182 (1979).
[15] G. Ehlers *et al.*, Phys. Rev. B **73**, 174429 (2006).